Fracture Mechanics of Concrete Structures, de Borst et al (eds) © 2001 Swets & Zeitlinger, Lisse, ISBN 90 2651 825 0

Shear behavior in fracture process zone of concrete

Y.Shinohara
Structural Engineering Research Center, Tokyo Institute of Technology, Tokyo, Japan

ABSTRACT: The primary purpose of this experimental investigation is to obtain the shear response in a cracked concrete, and to accumulate the necessary information that applies to nonlinear finite element analysis. A biaxial testing device, with which the vertical and horizontal load as well as displacement can be independently controlled by closed-loop servo systems, has been developed in order to establish the shear behavior in cracked concrete. The shear tests on specimens containing narrow cracks (fracture process zone introduced by the tensile test in displacement control) have been carried out maintaining either normal displacement or load across the crack surface constant. The relation of normal and shear loads to crack opening and sliding displacements was discussed and distinguished by the boundary conditions of the normal direction across the crack surface. Several expressions which give shear retention factor and so on, have been derived from the experimental results.

1 INTRODUCTION

The non-linear behaviors of concrete structures are mainly due to the occurrences and the propagations of cracks in them. It has now been widely accepted that a fracture process zone is formed at the crack tip in a concrete structure because of the heterogeneity inherent in concrete. To promote the study for the mechanical behavior in a concrete structure, and to develop a new material and predict its properties, it is important to make clear the crack behaviors and the mechanical properties in fracture process zone.

Tension softening models have been studied extensively worldwide, and incorporated in many finite element codes. Many structural problems, however, require more generally applicable models because the behavior of a structure is rarely confined to the pure tension. Most cracks in concrete structures are initiated first by the maximum principal stress, and propagate under subsequent shear and transverse compression or tension. Van Mier (1991) have studied the behavior in a fracture process zone under combined tensile/compressive and shear loading, and tried to derive constitutive equations relating normal and shear stresses to crack opening and sliding displacements. The necessary information on the behavior of small crack openings under shear seems to be yet lack.

The primary purpose of this experimental investigation is to obtain the shear response in a fracture process zone that the stress can still be transferred in spite of the damage, and to accumulate the necessary information that applies to nonlinear finite element analysis. Since the mixed mode loading in concrete structures is a consequence of the presence of a crack due to principal tensile stresses and subsequent rotation of the principal stress direction, testing methods require that a small crack can be generated first under pure tension and that shear can be applied in a second stage, as stated by Van Mier (1991). In this paper, the shear tests on specimens containing narrow cracks introduced by the tensile test in displacement control have been carried out under the boundary conditions maintaining either normal displacement or load across the crack surface constant. The relation of normal and shear loads to crack opening and sliding displacements was discussed on the basis of the boundary conditions of the normal direction across the crack surface.

2 DEFORMATION OF A SQUARE DOUBLE-EDGE NOTCHED SPECIMEN

The deformation of a square double-edge notched specimen used in this test was first calculated by linear elastic fracture mechanics and finite element method and used to verify the test results. When a double-edge-notched plate is loaded by a tensile force P or a bending moment M, as illustrated in Figure 1, incremental displacements which are due to the introduction of a notch are obtained from the

increase of strain energy due to the notch (Griffith approach), and using Benthem's (1973) approximations they are given by

$$\Delta u = \frac{P\pi}{BE}\int_0^{\xi}\left\{1.122(1-\frac{1}{2}\xi)-0.015\xi^2+0.091\xi^3\right\}^2\cdot\xi\cdot\frac{1}{1-\xi}d\xi \quad (1)$$

$$\Delta\theta=\frac{9M\pi}{bBE}\cdot\int_0^{\eta}(\frac{4}{3\pi}\cdot(1+\frac{1}{2}\eta+\frac{3}{8}\eta^2+\frac{5}{16}\eta^3)-0.470\eta^4+0.663\eta^5)^2\cdot\frac{1}{a^3}\cdot(b-a)\cdot da \quad (2)$$

Figure 2 shows finite element meshes and boundary conditions used to predict principal stresses and their directions in the specimens that are free of any nonlinear area such as narrow cracks.

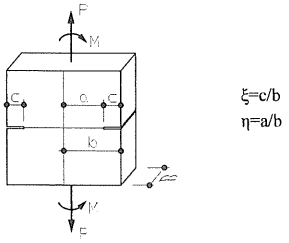

Figure 1. Deformations of a double-edge-notched plate by linear elastic fracture mechanics (LEFM)

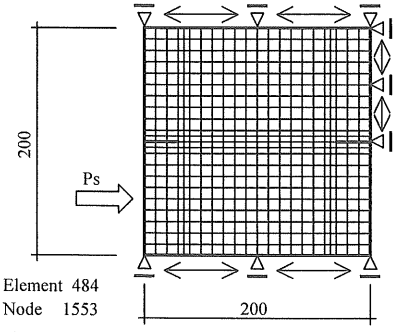

Figure 2. Finite element mesh and boundary conditions

3 EXPERIMENTAL PROCEDURES

3.1 *Preparation of specimens*

Experiments have been conducted on the mortar and the concrete with a maximum aggregate size of 5 mm and 20 mm respectively to study the effect of material structure on the shear behaviors. The mix proportions are given in Table 1. The ordinary Portland cement is used without any admixture. The fine aggregate is a siliceous sand which has a fineness modulus of 2.90 and a specific gravity of 2.52. The coarse aggregate is a semi-rounded gravel which has a bulk density of 16.9 kN/m^3, a fineness modulus of 6.67 and a specific gravity of 2.60. One plate of size 880×200×100 mm^3 and six cylinders of 100 mm diameter were cast in steel molds at the same time.

Table 1. Mix proportion

Specimen	W / C	Water kg/m^3	Cement kg/m^3	Aggregate kg/m^3	Sand kg/m^3
Concrete	0.55	194	353	1066	651
Mortar	0.55	323	587	-	1174

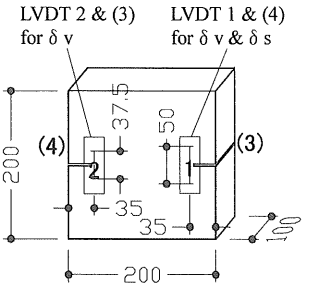

Figures in parentheses indicate rear face

Figure 3. Dimensions of shear specimens and designations of displacements

About 24 hours after casting the plate and cylinders were removed from the moulds and cured under water maintained at 20 ℃. At an age of 21 days the plate was cut using a rotating diamond saw into four square specimens used in shear tests of size 200×200×100 mm^3. The double-edge-notch that was 30 mm in depth and 3 mm in width was introduced at half height to facilitate displacement controlled tensile tests, as shown in Figure 3. After that all specimens were stored in a curing room maintained at 20 ℃ to dry until testing. The age at testing was always 29 to 32 days. The cylinders were used to determine the compressive strength, elastic modulus and splitting tensile strength.

3.2 *Testing Procedures*

A biaxial loading device, with which the vertical and horizontal load as well as displacement can be independently controlled by closed-loop hydraulic systems, has been developed in order to investigate the shear behaviors of the specimens containing narrow cracks (0-0.8 mm), as shown in Figures 4 and 5. The shear tests have been carried out keeping either normal displacement or load across the crack surface constant to study the effect of boundary conditions. The conducted test series are summarized in Table 2 where figures in parentheses indicate the number of specimens tested under cyclic loadings. The upper and lower sides of a specimen were carefully prepared and glued into steel plates bolted to roller supports using epoxy adhesive agency on the day before testing, and a small compressive force of 5 kN was applied to provide firm adhesion until testing. A gap

between the specimen and the shear platen was filled up with super high early Portland cement. The boundary conditions of specimens were adjusted to allow for the necessary movements in the vertical and horizontal directions during a test. Direct tension tests to introduce the prescribed narrow cracks (the fracture process zone) are required to eliminate occurrence of sudden failure near the peak load and to obtain a complete load-displacement curve. This was accomplished by a displacement-controlled test with a rate of 1.2 μm/min using the 1000 kN fatigue testing machine. The average vertical displacement calculated from LVDT 2 and 3 (Fig. 3) that were fixed in diagonally opposite positions of the specimen was used as the feedback signal in the servo controlled system. These LVDTs have a gage length of 37.5 mm, a linear stroke of ±2.5 mm and a resolution of 0.5 μm with a nonlinearity of 0.1 %. In the case of shear tests under constant crack opening, after introducing a prescribed crack opening, it was kept constant, and the shear load was applied in displacement control with a rate of 30 μm/min using the 200 kN actuators. For shear tests under constant vertical load, after loading the specimen up to a prescribed crack opening, the test control was changed from displacement to load and it was unloaded to –1 kN (–0.07 Mpa). Subsequently, the shear load was applied in a manner similar to shear tests under constant crack opening while the vertical load was kept constant at –1 kN. The shear displacement was defined as the average horizontal displacement of biaxial LVDT 1 and 4 (Fig. 3) that have a gage length of 50 mm, a linear stroke of ±3 mm and a resolution of 1.0 μm with a nonlinearity of 0.5 %. The vertical and shear loads were measured using load cells with 0.04 kN and 0.1 kN sensitivity respectively.

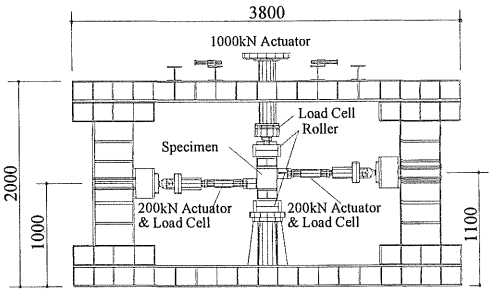

Figure 4. Biaxial testing device

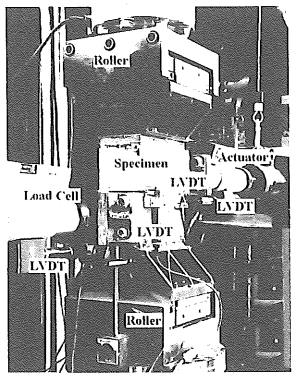

Figure 5. Loading apparatus

Table 2. Test series and the number of tested specimens

Specimen	Control Method	Initial Crack Width δ_0 (mm)						
		0	.05	0.1	0.2	0.4	0.6	0.8
Concrete (Max. Grain Size 20 mm)	Displacement (δ_v=δ_0)	4 (2)	—	1 (2)	3 (2)	3 (2)	3 (2)	2 (2)
	Load (P_v=–1 kN)	3 (2)	— (2)	1 (2)	2 (2)	3 (2)	(2)	(2)
Mortar (Max. Grain Size 5 mm)	Displacement (δ_v=δ_0)	2 —	— —	1 —	3 —	1 —	1 —	— —
	Load (P_v=–1 kN)	2 —	— —	— —	2 —	— —	— —	— —

Figures in parentheses indicate specimens under cyclic loading

4 RESULTS AND DISCUSSIONS

4.1 *Uniaxial tension behavior before applying shear load*

The average material properties obtained from compressive tests of cylinders are shown in Table 3, where the shear modulus is calculated from the secant modulus and the Poisson's ratio of one-sixth.

An example of uniaxial tensile tests to intrroduce a prescribed crack opening is shown in Figure 6, which shows the tensile load (Pv) – vertical displacement (δv) curve and the shear load (Ps) – δv curve of a concrete specimen during tensile tests. When the vertical displacement was approximately 0.01 mm (①), the maximum load was reached. Subsequently the rapid softening started under dis-

Table 3. Average material properties from compressive tests

Specimen	Comp. Strength f_c(Mpa)	Secant Modulus $E_{1/3}$(Gpa)	Shear Modulus G_0(Gpa)
Concrete	34.8	28.8	12.3
Mortar	47.0	22.9	9.82

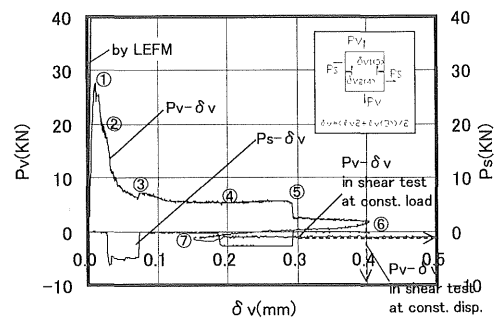

Figure 6. Pure tension behavior in producing a prescribed crack opening of 0.4 mm before applying shear load

placement-controlled test. The straight line in this figure is the prediction by linear fracture mechanics considered in section 2. The displacement of the specimen becomes greater than that of the prediction with increasing tensile load because the fracture process zone develops more rapidly by the effect of the bending. As can be seen from this figure, small shear load (0 to –6 kN) is also generated when the vertical displacements of δv1 and δv4 fluctuated sharply at discontinuous points (②,③,④,⑤) in the softening region. The difficulty of the uniaxial tensile tests on concrete specimens under deformation-controlled conditions arises from the eccentricity produced during tests. The eccentricity exists even before cracking of the specimen due to its heterogeneity. After cracking, the shape of the effective area is irregular, and the eccentricity of loading will be getting more severe, as shown by Shinohara (1995).

4.2 *Shear behavior under constant crack opening*

Figure 7 shows the shear load (Ps) versus shear displacement (δs) curve at the top and the vertical load (Pv) versus δs curve at the bottom during shear tests on concrete under a constant crack opening of 0.6 mm. Figure 8 shows the comparison of shear behaviors obtained from the individual specimens for the same crack opening of 0.2 mm. The deviation from the average behavior is slight for less than 0.4 mm

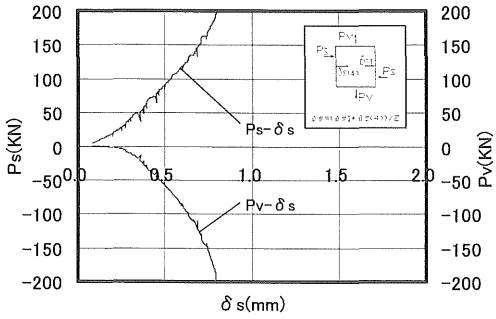

Figure 7. Shear behavior at constant crack opening of 0.6 mm

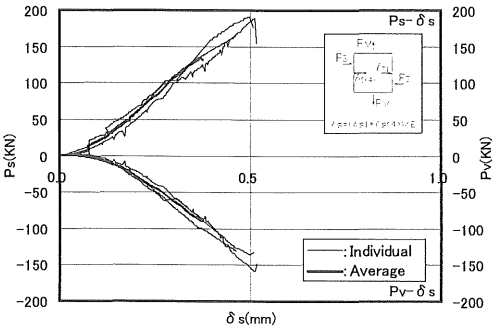

Figure 8. Deviation of results tested by same crack opening of 0.2 mm (concrete specimens)

crack openings. The differences among individual specimens are increasing when the crack opening is over 0.4mm because the shear behaviors depend greatly on the meandering path of rough cracks. It can be seen from Figures 6 to 8 that the vertical load had to be changed from tensile to compressive in order to keep the crack opening (δ_0) constant when shear is applied. The vertical load increases with increasing shear load and the state of stress in the specimen during the shear test is compression-compression. The biaxial strength is estimated above –200 kN (14 Mpa) that is the capacity of the actuators, and no secondary cracking is produced during these shear tests. The ratio of shear stress to restraining stress (Ps/Pv), i.e. the coefficient of friction in these tests is approximately 1.3. This result differs from one suggested by Paulay (1974), which showed a coefficient of friction of 1.7. In Paulay's tests, crack widths could not be controlled when the shear stress was in excess of 7 Mpa. This difference seems to be due to the complete prevention of increases in the crack opening up to higher stress levels, which requires larger restraining stress.

4.3 *Shear behavior under constant vertical load*

Figure 9 shows Ps versus δs curve at the top and the vertical displacement (δv) versus δs curve at the bottom for a concrete specimen with a precrack of 0.4 mm during shear tests under a constant vertical load of –1 kN. A shear displacement across the crack surface cannot occur at constant crack opening if the vertical load across the crack surface is constant. Because of rough surfaces of cracks, the shear displacement is always accompanied by an increase of the crack opening, that is, uplift in order to keep the vertical load constant. As can be seen from this figure, with an increase in the shear displacement, the vertical displacement gradually increases and the shear stiffness decreases up to the maximum shear load. After the peak load, the softening accompanied by rapid uplift and secondary cracks started. Despite the use of displacement control, this specimen failed in an unstable manner at position 10 in this figure.

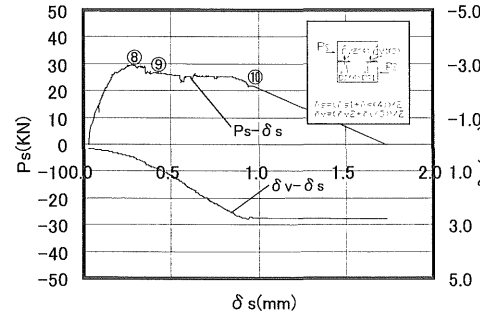

Figure 9. Shear behavior at constant –1 kN normal load

4.4 *Direction of crack propagation*

If specimens were not precracked for shear tests under constant vertical load, it was found that a diagonal cracking always nucleated and extended from the bottom of the right notch, as shown in the left of Figure 10. According to FEM analysis stated in section 2, the maximum principal stress occurred at the right notch tip and the direction normal to it is also shown in Figure 10. The initial crack propagated in the direction normal to the maximum principal stress. This means the shear failure may be caused by tensile stress. The crack propagation is due to the tensile stresses and perpendicular to the direction of the principal stress. With further increasing shear displacement, the second diagonal crack ran from the top of the left notch, so that a compressive strut eventually formed in the specimen. In that case, the compressive shear load would be carried by the intact part between two diagonally overlapping cracks, as shown in the right of Figure 10.

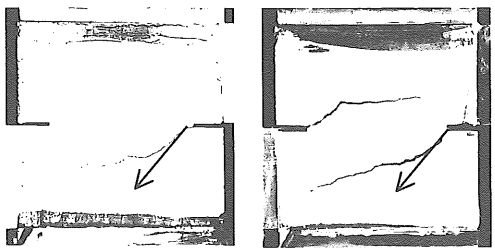

Figure 10. Crack propagation behaviors for two different specimens without a precrack and predictions by FEM

4.5 *Relations between load increment and crack displacements*

After a crack has developed, shear and vertical loads act on the crack under their displacements. The relation between load increments and crack displacements can be given in Figure 11, where v refers to the direction vertical to the crack and s refers to the

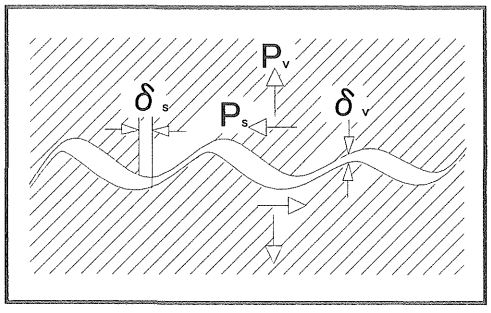

Figure 11. Shear and vertical displacements in crack faces under loads

$$\begin{Bmatrix} \Delta P_V \\ \Delta P_S \end{Bmatrix} = \begin{bmatrix} K_{11} & K_{12} \\ K_{21} & K_{22} \end{bmatrix} \begin{Bmatrix} \Delta \delta_V \\ \Delta \delta_S \end{Bmatrix} \quad (3)$$

shear direction parallel to the crack. The stiffness matrix K_{ij} reveals the fact that a vertical load causes vertical and shaer displacements and that a shear load causes also both displacement components. This factor is due to the roughness of the crack surfaces. Experiments have shown that $K_{12} \neq K_{21}$ i.e. the stiffness matrix is not symmetric which causes some numerical inconvenience. As Walraven (1987) has shown, K_{12} can be put to zero if $\delta s/\delta v < 2/3$. This is valid for most structural cases. K_{21} takes account of a decreasing shear stiffness with increasing crack width. If this phenomenon is formulated by making K_{22} crack width dependent, K_{21} can also put to zero. Then, the stiffness matrix Kij becomes symmetric and numerically simpler (Hordijk (1989)).

4.6 *Shear behavior due to crack width*

Figure 12 shows the shear load (Ps) versus shear displacement (δs) average curves at the top and the vertical load (Pv) versus shear displacement average curves at the bottom for a number of shear tests with six different crack openings. From this figure the shear stiffness decreases with increasing initial crack width as was expected. The shear stiffness and an

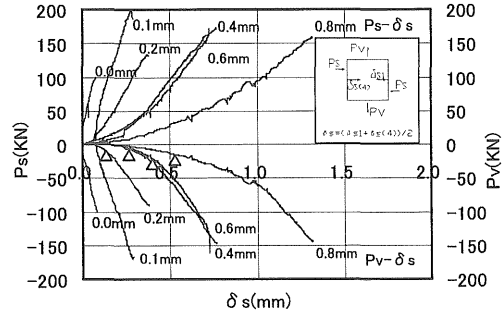

(1) Concrete

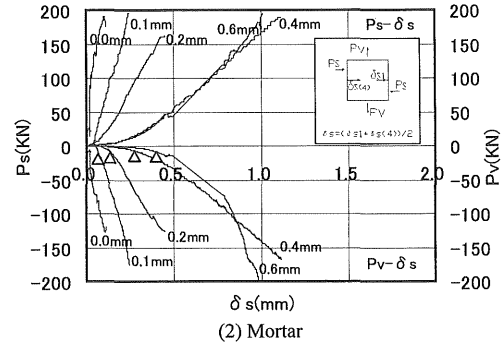

(2) Mortar

Figure 12. Ps-δs and Pv-δs curves for different crack openings

increase of vertical load are very small for small shear displacement of a wide crack to slide between crack surfaces. The shear stiffness increases with increasing shear displacement because the rough crack surfaces become to have firm contact each other and the aggregate interlock works gradually. The shear displacements K_{12} can be put to zero, as suggested by Walraven (1987), are also indicated by triangular marks in this figure. Since the vertical loads slightly increase up to triangular marks and increase rapidly beyond them, Walraven's suggestion would be also valid for very small crack openings. There seems no significant difference between concrete and mortar when the crack opening is less than 0.4 mm because of the close confinement normal to the crack plane. This reflects the fact that mortar specimens have also rough crack surfaces, though they are smoother than those of concrete.

4.7 *Decrease in shear stiffness due to crack width*

Figure 13 shows shear retention factors (β) as function of the initial crack opening (δ_0). The shear stiffness (Ps/δs) is defined as the secant modulus between 20 kN and 70 kN shear loads for constant crack opening tests, and as the tangent modulus at a shear load of 10 kN for constant vertical load tests. From this definition, the shear stiffness can be calculated from relatively linear parts of Ps–δs curves for all specimens. The shear stiffness for specimens with no precrack was largely scattered (±20%) because the shear displacement was infinitesimally small. Therefore, the shear stiffness of the intact specimen was calculated from shear modulus in Table 3 and used to estimate shear retention factors. The calculated shear stiffness for concrete and mortar specimens with no precrack are 3450 kN/mm and 2750 kN/mm respectively. The expression which gives shear retention factor has been derived on the basis of test results,

$$\beta = 1/(1 + a\delta_0) \tag{4}$$

where a is an experimental constant indicated in this figure. The expression proposed by Bazant (1980) is also shown in this figure for comparison. It can be seen that the shear stiffness is steeply reduced in small crack openings. As mentioned in Figure 12, the difference between concrete and mortar is not very pronounced for small crack openings. As a result, shear retention factors depend greatly on secant

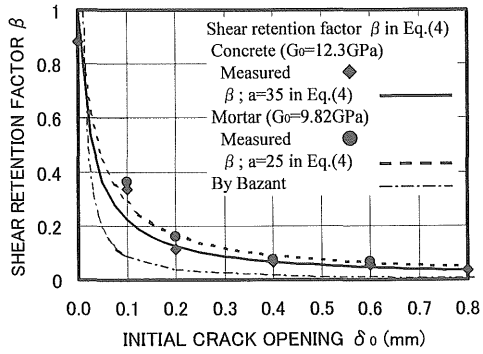

(1) Shear test at constant crack opening

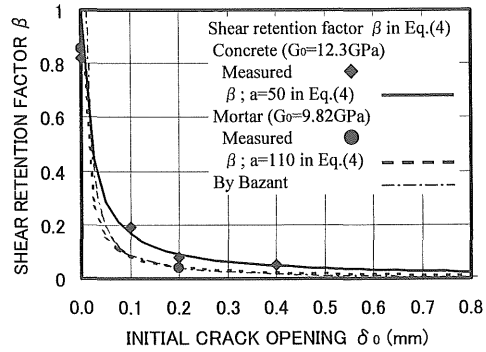

(2) Shear test at constant vertical load

Figure 13. Decrease of shear stiffness with increasing initial crack openings

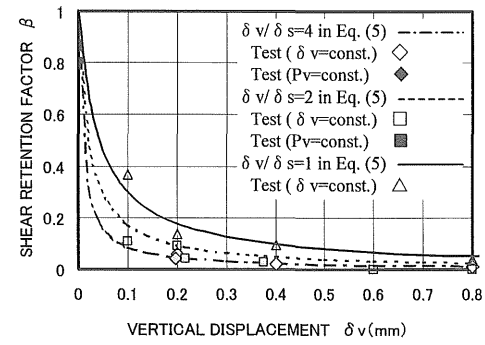

(1) Concrete

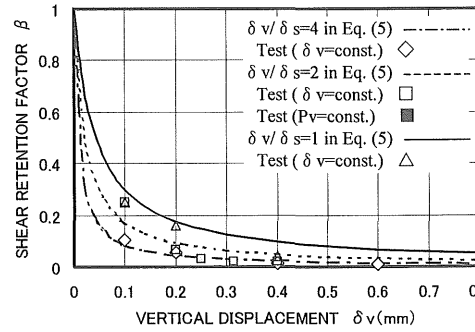

(2) Mortar

Figure 14. Decrease of shear stiffness with increasing vertical displacement and δv/δs

modulus used to calculate the shear stiffness of no cracked specimens. In the case of shear tests at constant vertical load, since the sliding accompanied by uplift seems to be prevalent failure mechanism, the shear retention factor of concrete, which has rougher crack surfaces, is generally higher than that of mortar. Bazant's expression gives smaller shear retention factors because it was probably derived for small shear displacements and not based on shear tests in fracture process zone.

As can be seen from Figure 12, the shear stiffness depends not only on crack openings (δv) but also on shear displacements (δs), so that a rather suitable expression considered to be a function of δv/δs is also proposed as follows:

$$\beta = 1/(1 + p\delta_v) \tag{5}$$

$$p = 1 + 21(\delta_v / \delta_s) + 1.5(\delta_v / \delta_s)^2 \tag{6}$$

The shear stiffness at shear displacement δs for a certain δv/δs was computed from the difference in shear loads between δs−0.025mm and δs+0.025mm. The same expression is used for concrete and mortar because there is no discernible difference between them. Figure 14 shows eq. (5) for three ratios of δv/δs together with experimental results. The larger the ratio δv/δs the more pronounced is the decrease. This means that the shear stiffness is very small for small shear displacements of a wide crack as mentioned in Figure 12. The stiffness is larger if the ratio δv/δs decreases by increasing shear displacement. This ratio shows the extent to which the aggregate interlock has an influence on the shear stiffness.

4.8 *Decrease in vertical load at constant crack opening due to crack width*

From the relations between vertical loads (Pv) and shear displacements (δs) in Figure 12, Pv produced during shear tests at constant crack opening also decreases with increasing crack openings. To investigate the effect of crack opening on Pv, K_{12} in Equation (3), which means ΔPv/Δδs if Δδv=0 (i.e. δv is constant), are plotted in Figures 15 and 16 as function of the initial crack opening (δ_0). The vertical axis shows the ratio of K_{12} for precracked specimens to K_{12} for intact specimens, which are 1600 kN/mm and 1450 kN/mm for concrete and mortar respectively. The methods for evaluating K_{12} were basically the same as those discussed in shear retention factors. The equations (7) and (8) which give a decrease in K_{12} due to initial crack openings have been also proposed and shown in Figures 15 and 16. As can be seen from these figures, K_{12} also decreases

$$\alpha = 1/(1 + b\delta_0) \tag{7}$$

$$\alpha = 1/(1 + q\delta_0) \tag{8}$$

$$q = 1 - 7.5(\delta_0 / \delta_s) + 19(\delta_0 / \delta_s)^2 \tag{9}$$

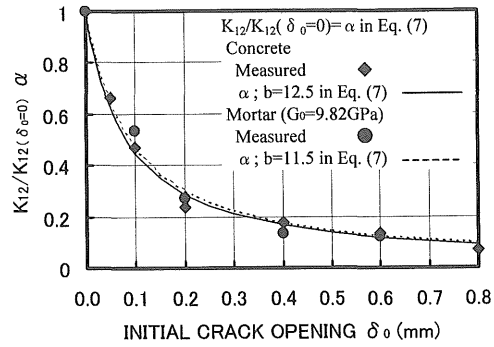

Figure 15. Decrease of α with increasing initial crack openings

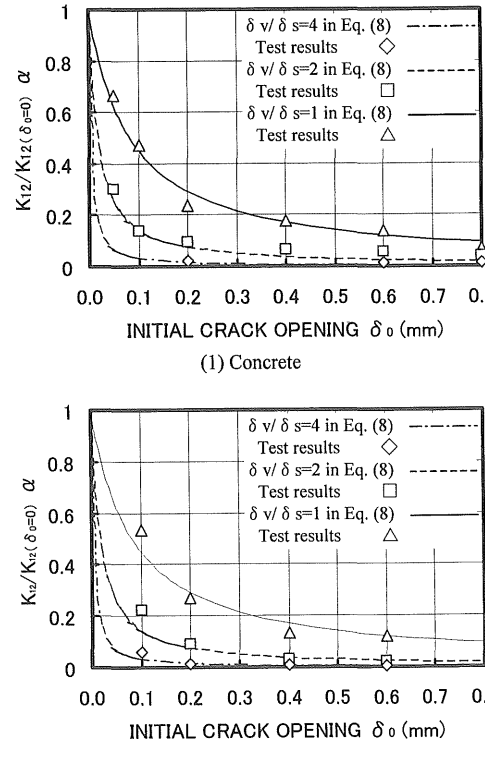

Figure 16. Decrease of α with increasing initial crack openings and δv/δs

with increasing initial crack openings in a manner similar to shear retention factors. However, the decrease rate is not so steep in K_{12} as in shear retention factors since K_{12} for intact specimens is approximately the half of the shear stiffness for specimens not containing any crack.

Eqs. (5) and (8) are valid for 0≤δv≤0.8 mm and 0≤δs≤1.0 mm.

4.9 *Shear behaviors under cyclic loading*

The experimental investigations to obtain the cyclic shear response have been also conducted on concrete specimens containing small crack openings of 0 to 0.8 mm. The typical shear behavior for cyclic shear tests under a constant crack opening of 0.2 mm is shown in Figure 17. While the tensile shear load was always applied up to 10 kN to avoid the fracture of adhesives, the compressive shear load was increased with the cycles in steps of −50 kN and then reduced. There are a number of characteristic features exhibited by these results. The envelope of Ps–δs drawn around the increasing displacement portion of the curves for the subsequent cycles lies entirely within the spread of results from specimens subject to monotonically increasing displacement. The first loading to −50 kN is different in character from later loadings to that same load. During the first loading the load gradually increases, whereas it rapidly increases after larger sliding displacements during subsequent loadings. This is probably due to the damage and the consolidation in a crack surface.

Figure 18 shows the cyclic shear response for a specimen with a precrack of 0.2 mm under a constant vertical load of −1 kN. The compressive shear load was turned back to the tension when the crack

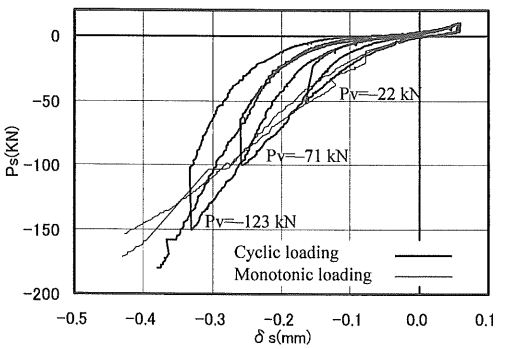

Figure 17. Cyclic shear response obtained from a test under constant crack opening of 0.2 mm

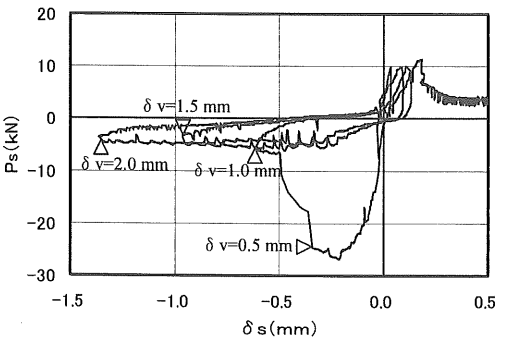

Figure 18. Cyclic shear response of a specimen containing initial crack of 0.2 mm at constant −1 kN normal load

opening has reached 1.0 mm, 1.5 mm and 2.0mm. A compressive strut which was similar to that shown in Figure 10 but more slender, was developed in the specimen with a precrack of 0.05 mm. This specimen lost most of its strength by breaking the strut instead of sliding and uplifting in rough cracks.

5 CONCLUSIONS

To study the shear behavior in a fracture process zone, the shear tests have been conducted on specimens containing narrow cracks under the boundary conditions maintaining either normal displacement or load across the crack surface constant. The relations of normal and shear loads to crack opening and shear displacements were discussed on the basis of two boundary conditions and loadings. Some characteristic features of the cyclic shear response were found by comparison with the response under monotonically increasing loading.

The shear tests have been further advanced to study the effect of confining pressures across the crack surface. The confining pressure is all the time estimated by reinforcement ratio, yield strength of reinforcement, slip between concrete and reinforcement, and automatically applied on crack surfaces by closed-loop servo systems.

ACKNOWLEDGEMENTS

I wish to acknowledge the experimental assistance of Ms. M.Kaneko, Mr. N.Takata, Mr. H.Muronaka, Ms. S.Ishitobi and Mr. K.Kawamichi. This research was supported by Grant-in-Aid for Scientific Research from the Ministry of Education in Japan.

REFERENCES

Bazant, Z. P. & Gambarova, P. 1980. Rough cracks in reinforced concrete. *J. Struct. Div. (ASCE)* Vol.106, No. ST4: 819-842

Benthem, J.P. & Koiter, W.T. 1973. Asymptotic Approximations to Crack Problems. *Methods of Analysis and Solutions of Crack Problems*: 131-158

Hordijk, D. A., Van Mier, J. G. M. & Reinhardt, H. W. 1989. Material properties. In L. Elfgren (ed.), *Fracture Mechanics of Concrete Structures*: 67-127: Chapman and Hall

Paulay, T. & Loeber, P. J. 1974. Shear transfer by aggregate interlock. *Special Publication SP 42-1, ACI*: 1-15

Shinohara, Y. , Abe, T. & Furumura, F. 1995. Effect of bending deformation upon tensile strength of concrete. *Report of RLEM Tokyo Institute of Technology* No. 20: 1-11

Van Mier, J. G. M., Nooru-Mohamed, M. B. & Timmers, G. 1991. An experimental study of shear fracture and aggregate interlock in cementbased composites. *HERON* Vol. 36, No. 4: 1-104

Walraven, J. C. & Keuser, W. 1987. The shear retention factor as a compromise between numerical simplicity and realistic material behavior. *Darmstadt Concrete* Vol. 2: 221-234